EUROPEAN ORGANIZATION FOR NUCLEAR RESEARCH

MEASUREMENT OF THE TOTAL PROTON-PROTON CROSS-SECTION AT THE ISR*)

S.R. Amendolia, G. Bellettini**), P.L. Braccini, C. Bradaschia, R. Castaldi†), V. Cavasinni, C. Cerri**), T. Del Prete, L. Foa**), P. Giromini, P. Laurelli, A. Menzione, L. Ristori, G. Sanguinetti and M. Valdata

Istituto Nazionale di Fisica Nucleare, Sezione di Pisa
Istituto di Fisica dell'Università, Pisa
Scuola Normale Superiore, Pisa

G. Finocchiaro, P. Grannis**), D. Green, R. Mustard and R. Thun

State University of New York
Stony Brook, New York

ABSTRACT

We present the first results of a measurement of the total cross-section σ_T in proton-proton collisions at equivalent laboratory momenta between 291 and 1480 GeV/c at the CERN Intersecting Storage Rings (ISR). The method is based on the measurement of the ratio of the total interaction rate and the machine luminosity. The data show an increase of about 10% in σ_T in this energy interval.

Geneva - February 1973
(Submitted to Physics Letters)

---

*) Work supported in part by the Consiglio Nazionale delle Ricerche of Italy, and by the National Science Foundation, USA.

**) These authors have held CERN visiting scientist positions.

†) Present address: State University of New York, Stony Brook, New York.

The simplest and most fundamental measure of the size of the proton as observed in very high energy p-p collisions is the total cross-section. The lower energy accelerator data have resulted in the expectation that σ_T should remain essentially constant through the ISR energies, and much of the phenomenological description of strong interactions in the ISR range has been based on the notion that we have nearly reached the energy-independent regime of hadron physics. In this paper we report a measurement of σ_T at four energies and find that there is an appreciable increase between 291 and 1480 GeV/c equivalent laboratory momentum.

At a machine with two colliidng beams, one cannot measure σ_T with a traditional transmission experiment. We instead find σ_T from the detected rate R_T of all interactions through the expression

$$R_T = \sigma_T L \ , \tag{1}$$

where L is the luminosity of the beams. The luminosity represents the overlap of the two beam fluxes in the intersection region, and replaces the product of beam intensity times number of targets/cm^2 in a conventional transmission experiment. In terms of the ISR parameters,

$$L = \frac{I_1 I_2}{c\ e^2\ \mathrm{tg}\ \frac{\alpha}{2}} \cdot \frac{1}{h_{eff}} \ , \tag{2}$$

where I_1 and I_2 are the beam currents, e is the charge of the proton, c the velocity of light, and α the crossing angle of the two beams. The effective height h_{eff} is defined in terms of integrals over the direction (vertical) perpendicular to the plane of the two beams, as

$$\frac{1}{h_{eff}} = \frac{\int \rho_1(z)\ \rho_2(z)\ dz}{\int \rho_1(z)\ dz \int \rho_2(z)\ dz} \ . \tag{3}$$

Here ρ_1 and ρ_2 are the beam densities as a function of z, the vertical coordinate. Inasmuch as all parameters in Eq. (2) except h_{eff} are known or measured during ISR operation to better than 0.1%, the determination of h_{eff} becomes the most delicate task in measuring L.

In the present letter, a brief description of the experimental apparatus and most relevant information on the procedure followed to measure σ_T are given. More details, both on the detectors and on the data reduction, can be found in a forthcoming paper[1].

The general layout of the experiment is shown in Fig. 1. The basic trigger requires at least one charged particle in cones surrounding each beam emerging from the interaction region. Each arm of the apparatus consists of hodoscopes H_1, H_2, H_3, H_4. Hodoscopes H_1 and H_2 are in coincidence and detect particles produced at angles $4^\circ \lesssim \theta \lesssim 30^\circ$. In a similar way, the coincidence of H_3 and H_4 covers angles $0.8^\circ \lesssim \theta \lesssim 7^\circ$. Each hodoscope consists of eight triangular counters, dividing the total azimuth into octants (Fig. 2a).

Two large-angle hodoscopes (L and L_s) surround the interaction region and cover the angular interval from $\sim 40^\circ$ to 90° over nearly the full azimuth (see Figs. 1 and 2b). In order to detect those events in which the charged particles are emitted at $\theta \gtrsim 40^\circ$ in one hemisphere, the coincidence $(L \cdot L_s)$ is used in the trigger. This signal is set in coincidence with one of the forward cones and added to the main trigger; by symmetry one knows the contribution of these large-angle particles in coincidence with the other cone.

The trigger is completed by small hodoscopes (TB) on each arm, positioned downstream of hodoscope H_4 in the region where the vacuum pipe has narrowed to an elliptical cross-section (see Fig. 2c). These hodoscopes are treated logically as small-angle elements of $(H_3 \cdot H_4)$.

In order to measure the emission angle of the produced particles, used to calculate the fraction of events lost by the trigger (see below), two additional hodoscopes $H_2\theta$ and $H_4\theta$ are set behind the trigger hodoscopes H_2 and H_4. The structure of these counters is shown in Fig. 2d. The L-hodoscope is also split into approximate θ-bins (see Fig. 2b).

When a trigger occurs, the information pertinent to an event is transferred to an on-line computer via a CAMAC data acquisition system. This information includes a bit (fired or not fired) for each counter of the hodoscopes, clock readings of live time, and several digitized time-of-flight (TOF) differences between hodoscopes ($H_4^{left} - H_4^{right}$, $H_4^{left} - H_2^{right}$, $H_2^{left} - H_4^{right}$, $H_2^{left} - H_2^{right}$, $H_4^{left} - L$, $H_2^{left} - L$). The fast logic is inhibited during data acquisition. The event rate entering into the cross-section was computed as the inverse of the average live time before a beam-beam event was recorded.

The resolving time of the main trigger was kept rather wide, ±30 nsec, and accepted an appreciable amount of background events due to jets of secondaries generated in beam-gas or beam-pipe interactions and accompanying the two beams. The separation of beam-beam events from single-beam background was obtained by analysing the previously mentioned TOF distributions, in which background events were concentrated in peaks well separated from those of beam-beam events. The shapes of the TOF spectra for background events were measured in separate runs with only one beam circulating in the machine. These spectra were normalized to the background peaks in the beam-beam runs and subtracted. We have checked the accuracy of the background subtraction by altering the procedure for extracting events from the various TOF spectra.

A flat background of less than 1% due to accidental hodoscope counts has been subtracted from the sample. The loss of good events owing to accidental start or stop of the TOF circuits was monitored in test runs taken in normal beam conditions, but triggering the electronics with a pulse generator. This loss was typically 1% and was added to the measured beam-beam rate.

Because of the central importance in our experiment of knowing the luminosity, we now discuss three independent approaches to the determination of h_{eff}, related to L by Eq. (2).

Before each data-taking run, three separate sets of scintillator monitors selecting different samples of beam-beam events were calibrated to give h_{eff} by the Van der Meer method[2]. In analogy with Eqs. (1) and (2)

$$R_M = \frac{K_M I_1 I_2}{h_{eff}} , \tag{4}$$

where R_M is the monitor rate of beam-beam events and K_M is the calibration constant. The Van der Meer (VDM) method consists in displacing the beams vertically with respect to each other and measuring R_M as a function of relative beam displacement δ. The value of $h_{eff}(t = 0)$ is then given as the ratio of the area under the displacement curve to the rate at the top of the curve, so that

$$K_M = \frac{1}{I_1 I_2} \int R_M(\delta)\, d\delta = \frac{1}{I_1 I_2} R_M^{top}\, h_{eff}(t = 0) . \tag{5}$$

The area under the displacement curve was obtained by numerical integration and also by fitting the data with simple functions such as a Gaussian The calibration constants were insensitive to within 1% to the method used to calculate the area. The h_{eff} value at any later time was obtained from the measured time dependences of R_M and I_1, I_2 and Eq. (4). The values obtained from our different monitors agreed to within 1%.

In order to check the displacement scale used in the Van der Meer method, we have employed a counter-spark chamber telescope, positioned in the horizontal plane, viewing the intersection region at 90° from inside the ISR rings. Nearly horizontal tracks can be projected back to the vertical plane at the beam centre. We have displaced the two beams equally in the same direction and measured the centre of the beam-beam profile. In addition, we have displaced a single beam through a dilute gas of titanium atoms evaporated from a source near the interaction region and have determined the centre of the distribution. These measurements give for the ratio of spark chamber scale to ISR scale 1.012 ± 0.010 and 1.000 ± 1.012, respectively. We thus assign an energy-independent normalization to the luminosity (and hence σ_T) of ±2%.

The second method of obtaining h_{eff} employs the spark chamber telescope. Using the titanium source, we measure the individual beam profiles $\rho_1(z)$ and $\rho_2(z)$ which from Eq. (3) yield h_{eff}. The trigger for this measurement selects a recoil proton from quasi-elastic beam-gas scattering with momentum greater than 600 MeV/c in the telescope and a small-angle particle along one of the beams. Events with particles elsewhere are rejected. The trigger topology allows identification of beam 1 (B1) or beam 2 (B2) events with a probability of misidentifying the beam of less than 3%. Values of h_{eff} obtained in this way are given in Table 1 and compared with the VDM values for the same time.

The third approach is provided by observing the beam-beam (BB) overlap $\rho_1(z)\rho_2(z)$ directly. The spark chambers are triggered during normal beam conditions by a pion of momentum greater than 190 MeV/c in the telescope and small-angle particles in both hemispheres to ensure BB events. This method is not fully independent of the second one, since one must know the relative widths and central positions of the two beams in order to extract h_{eff} from the observed BB overlap. The usual sequence of spark chamber runs was BB, B1,B2, and again BB. The widths and centres of B1 and

B2 profiles are used to calculate the correction factor, usually close to one, required to analyse the BB profiles. Table 1 gives h_{eff} values from the BB measurements.

The resolution in the vertical beam coordinate z in the spark chamber measurements is mostly due to multiple scattering in the vacuum pipe wall and in the chambers themselves. It is to a lesser extent due to the intrinsic chamber resolution and the track projection error across the beam width. These effects have been computed with detailed Monte Carlo calculations. The probable error in the resolution is estimated to be $\leq 10\%$, which causes a possible systematic error in spark chamber values of h_{eff} of $\leq 3\%$.

The listed errors in Table 1 for spark chamber measurements are statistical only, while those on the VDM method are not only statistical, but also include the uncertainties arising from fitting the VDM displacement curves. Agreement between spark chambers and VDM is generally within 3% and consistent with the errors. Only VDM values of h_{eff} have been used to obtain σ_T in this paper and have an estimated accuracy of $\pm 2\%$. The spark chamber measurements have a somewhat greater uncertainty but exclude the possibility of large (> 3%) errors in the luminosity.

The ratio of the measured rate of beam-beam interactions and the luminosity gives the partial cross-section detected by the apparatus. The fourth column of Table 2 shows the values obtained at incident beam momenta of 11.8, 15.4, 22.6, and 26.6 GeV/c.

In order to obtain the total cross-section, a correction must be made for events not accepted by the trigger. The most important loss is due to protons scattered elastically at angles smaller than the inner edge of the TB counters. It should be observed that such protons emitted towards the small-angle detectors can also fail to give a trigger, owing to multiple scattering and interactions in the pipes. The over-all loss was calculated with the Monte Carlo method and with known parameters of elastic scattering[3]. The results are given in column 5 of Table 2. Quoted errors are due to uncertainties in the elastic cross-section, in the geometry of detectors and interaction diamond, and in the model adopted to describe proton-pipe interactions.

A small fraction of inelastic events fail to trigger because the charged particles are all emitted towards the beam exit holes in H_4 or towards the gaps $30^\circ \lesssim \theta \lesssim 40^\circ$ between H_2 and L.

The loss of inelastic events due to charged particles directed inside the beam exit holes has been estimated by plotting the trigger rate as a function of the maximum angle of the produced prongs in either cone. The amount of elastic events contained in this sample was subtracted. The distribution of the remaining events was extrapolated to zero angle, and was used to calculate the loss inside the pipes. The result at the various energies is given in the sixth column of Table 2. The errors include an estimate of possible systematic effects. The loss of events due to all charged particles of one hemisphere being produced in the gap between H_2 and L has been studied and found to correspond to less than 0.05 mb at all momenta. This loss has been neglected.

The final values for σ_T are quoted in the seventh column of Table 2 and are shown in Fig. 3, together with values from Serpukhov[4] and NAL[5-7]. The errors correspond to root-mean-square addition of the errors on the entries of columns 4, 5, and 6 of Table 2. They are dominated by the 2% error taken for the luminosity determination. In addition, as explained before, we associate a ±2% over-all normalization error common to all momenta arising from possible systematic effects in the luminosity scale.

We note the increase in total cross-section of nearly 4 mb within the energy interval studied. These data are in excellent agreement with recently available measurements[8] at the ISR which employ the elastic cross-section and the optical theorem to obtain σ_T. They also agree at our lowest momentum with the highest energy data at NAL[7]. The existence of a rise in σ_T at energies above the ISR range has already been suggested from cosmic-ray measurements[9]. The possibility of rapidly rising total cross-sections at very high energies has been considered theoretically by Heisenberg[10], and by Cheng and Wu[11]. The presence of an energy dependence in σ_T indicates that if an asymptotic limit exists, it has not been reached at ISR energies, and points up the interest in extending all total cross-section measurements to higher energies.

We would like to thank all the people who have contributed to the success of this experiment, and in particular the ISR staff for the excellent operation of the machine and the CERN Directorate for their warm support. We appreciate the encouragement and the help in Italy given by Professors C. Villi and G. Stoppini, and the advice of Professors M.L. Good, J. Kirz and C.N. Yang in Stony Brook. The help of J. Renaud has been essential for the smooth running of the experiment. Our group technicians A. Bechini and G. Mugnai, and all technicians of the Physics Department of the University of Pisa, have given a decisive and essential contribution. Dr. G. Ciancaglini has led the design and installation of the counter hodoscopes with great enthusiasm and competence.

Table 1

Measured effective heights referred to a common time

Beam momentum (GeV/c)	Date (1972)	h_{eff} (mm)		
		Van der Meer method a)	Beam 1 and beam 2 profiles	Beam 1 - beam 2 overlap profile
11.8	14 Nov.	8.12 ± 0.14	8.11 ± 0.14	8.47 ± 0.30
15.4	18 Dec.	7.90 ± 0.08	7.60 ± 0.11	7.63 ± 0.13
22.6	15 Dec.	6.10 ± 0.12	6.12 ± 0.19	5.83 ± 0.08
26.6	19 Nov.	6.15 ± 0.09	6.42 ± 0.18	6.16 ± 0.12

a) There is a possible ±2% scale error common to all Van der Meer values.

Table 2

Summary of results on total cross-section

Beam momentum (GeV/c)	c.m. energy squared $(GeV)^2$	Equivalent lab. beam momentum (GeV/c)	Detected cross-section (mb)	Increment for elastic loss (mb)	Increment for inelastic loss (mb)	σ_T (mb)
11.8	548	291	38.66 ± 0.79	0.54 ± 0.10	0.10 ± 0.02	39.30 ± 0.79
15.4	932	496	39.93 ± 0.81	0.75 ± 0.10	0.17 ± 0.04	40.85 ± 0.82
22.6	2005	1068	40.69 ± 0.84	1.54 ± 0.15	0.34 ± 0.10	42.57 ± 0.86
26.6	2776	1480	40.53 ± 0.83	1.95 ± 0.20	0.50 ± 0.12	42.98 ± 0.84

REFERENCES

1) Pisa-Stony Brook Collaboration, "Total cross-section measurement at the ISR", submitted to Nuovo Cimento.

2) S. Van der Meer, CERN Internal Report ISR-PO/68-31 (1968), unpublished.

3) U. Amaldi, R. Biancastelli, C. Bosio, G. Matthiae, J.V. Allaby, W. Bartl, G. Cocconi, A.N. Diddens, R.W. Dobinson and A.M. Wetherell, submitted to Physics Letters.
G. Barbiellini, M. Bozzo, P. Darriulat, G. Diambrini-Palazzi, G. De Zorzi, A. Fainberg, M.I. Ferrero, M. Holder, A. McFarland, G. Maderni, S. Orito, J. Pilcher, C. Rubbia, A. Santroni, G. Sette, A. Staude, P. Strolin and K. Tittel, Phys. Letters 39 B, 663 (1972).

4) S.P. Denisov, S.V. Donskov, Yu.P. Gorin, A.I. Petrukhin, Yu.D. Prokoshkin, D.A. Stoyanova, J.V. Allaby and G. Giacomelli, Phys. Letters 36 B, 415 (1971).

5) J.W. Chapman, N. Green, B.P. Roe, A.A. Seidl, D. Sinclair, J.C. Van der Velde, C.M. Bromberg, D. Cohen, T. Ferbel, P. Slattery, S. Stone and B. Werner, Phys. Rev. Letters 29, 1686 (1972). (100 GeV/c data.)

6) G. Charlton, Y. Cho, M. Derrick, R. Engelmann, T. Fields, L. Hyman, K. Jaeger, U. Mehtani, B. Musgrave, Y. Oren, D. Rhines, P. Schreiner, H. Yuta, L. Voyvodic, R. Walker, J. Whitmore, H.B. Crawley, Z. Ming Ma and R.G. Glasser, Phys. Rev. Letters 29, 515 (1972). (200 GeV/c data.)

7) F.T. Dao, D. Gordon, J. Lach, E. Malamud, T. Meyer, R. Poster and W. Slater, Phys. Rev. Letters 29, 1627 (1972). (300 GeV/c data.)

8) See U. Amaldi et al., Reference 3.

9) G.B. Yodh, Yash Pal and J.S. Trefil, Phys. Rev. Letters 28, 1005 (1972).

10) W. Heisenberg, Kosmische Strahlung (Springer Verlag, Berlin, 1953), p. 148.

11) H. Cheng and T.T. Wu, Phys. Rev. Letters 24, 1456 (1970).

Figure captions

Fig. 1 : Schematic layout of the experiment. H_1, ..., H_4, counter hodoscopes, binned in ϕ-octants. $H_2\theta$, $H_4\theta$, counter hodoscopes comprising four quadrants split into θ-bins. L, double-layer counter hodoscope box (four planes of scintillator/lead/scintillator sandwich). L_S, small counter box (four counters) surrounding the intersection. TB, scintillation counters leaving minimum clearance for the beam pipes. Some additional monitor counters are not shown in the figure.

Fig. 2 : Schematic drawing of hodoscope counters.

a) H_1 hodoscope. Hodoscope H_2 is similar, but the ϕ-bins are rotated by $\pi/16$. Hodoscopes H_3 and H_4 are like H_1, H_2, but with no off-centre hole.

b) L-box. Only the first layer is shown. The second layer is behind it, with a lead plate in between.

c) TB counters.

d) θ-hodoscopes. The outer rings are split into octants, the inner rings into quadrants.

Fig. 3 : Plot of the results versus equivalent beam momentum. The Serpukhov (Ref. 4) and NAL (Refs. 5-7) data are shown for comparison.

□: Data of Ref. 4; ○ : Data of Refs. 5-7; ● : This experiment.

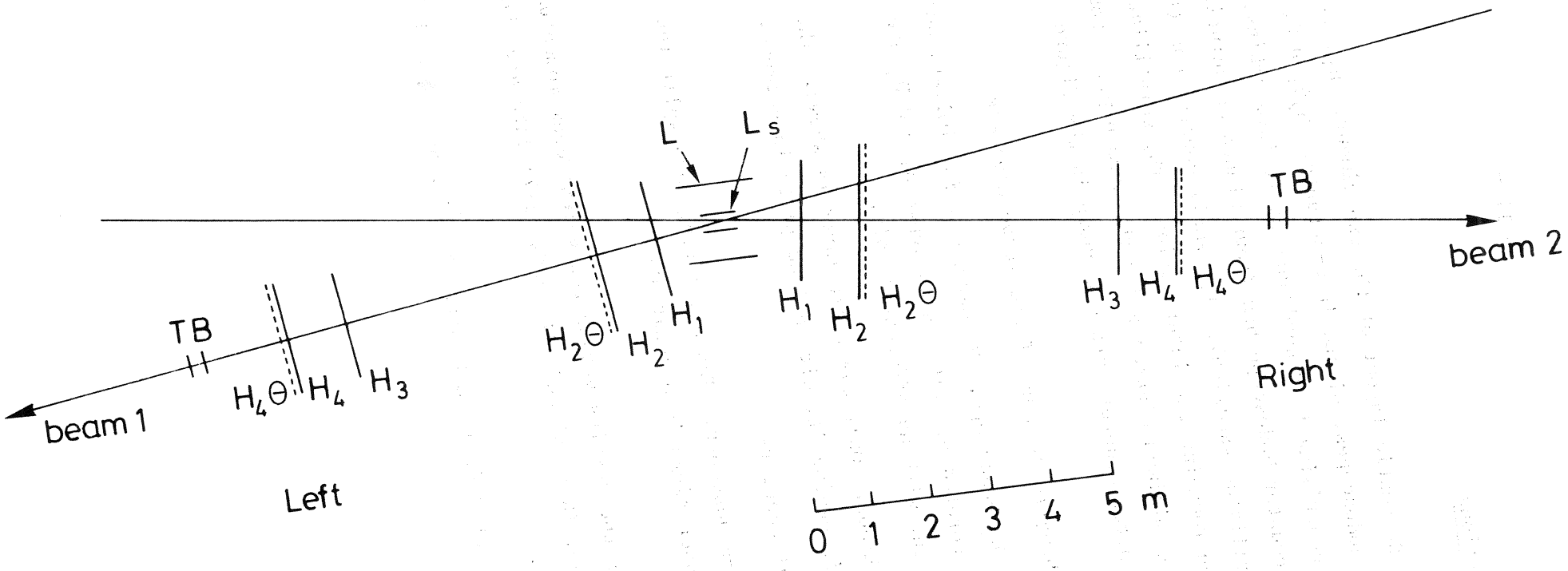
L
Ls
TB
beam 2
TB
H4Θ
H4
H3
H2Θ
H2
H1
H1
H2
H2Θ
H3
H4
H4Θ
beam 1
Left
Right
0 1 2 3 4 5 m

FIG.1

PISA - STONY BROOK

SKETCH OF COUNTERS OF TOTAL CROSS-SECTION EXPERIMENT

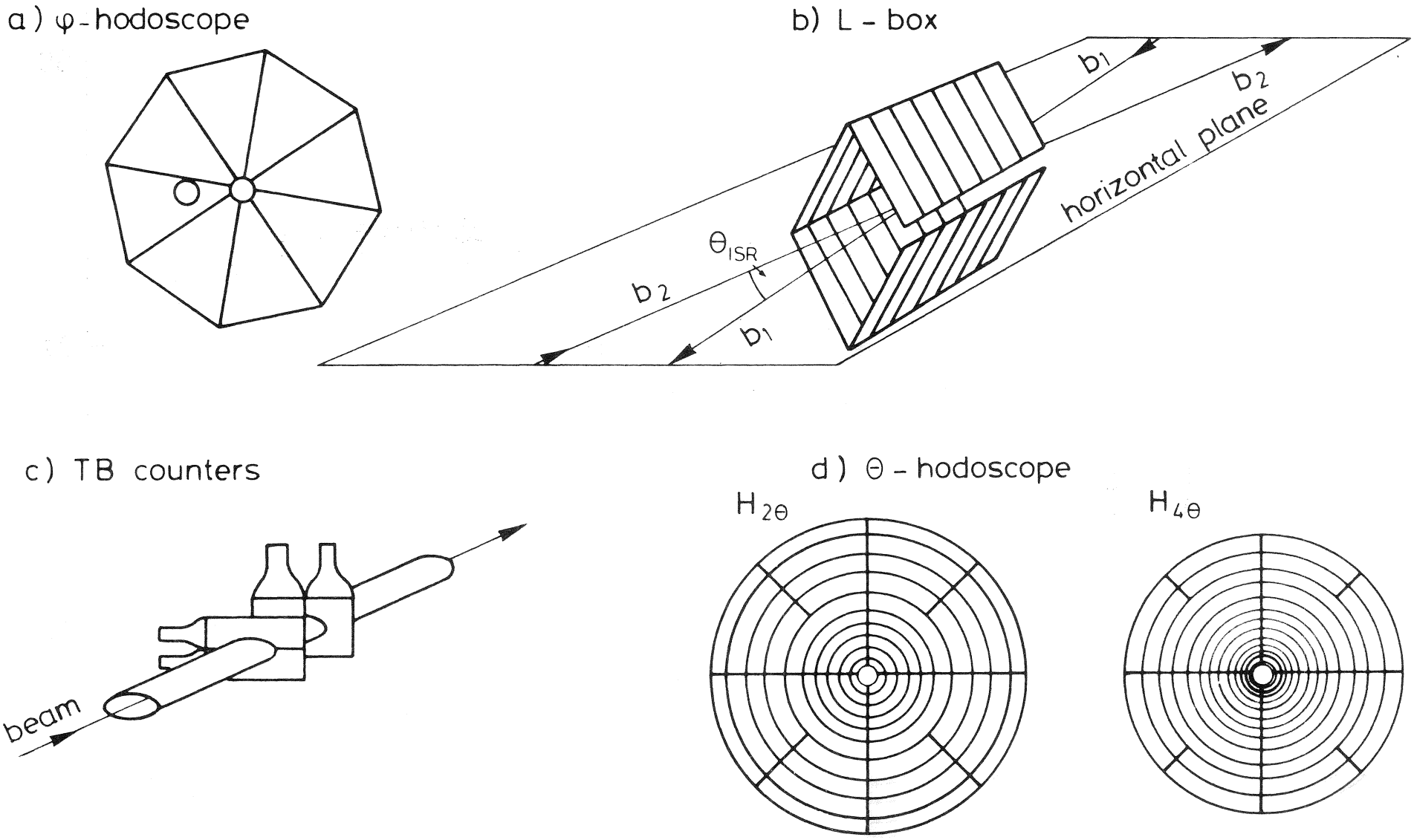

FIG. 2

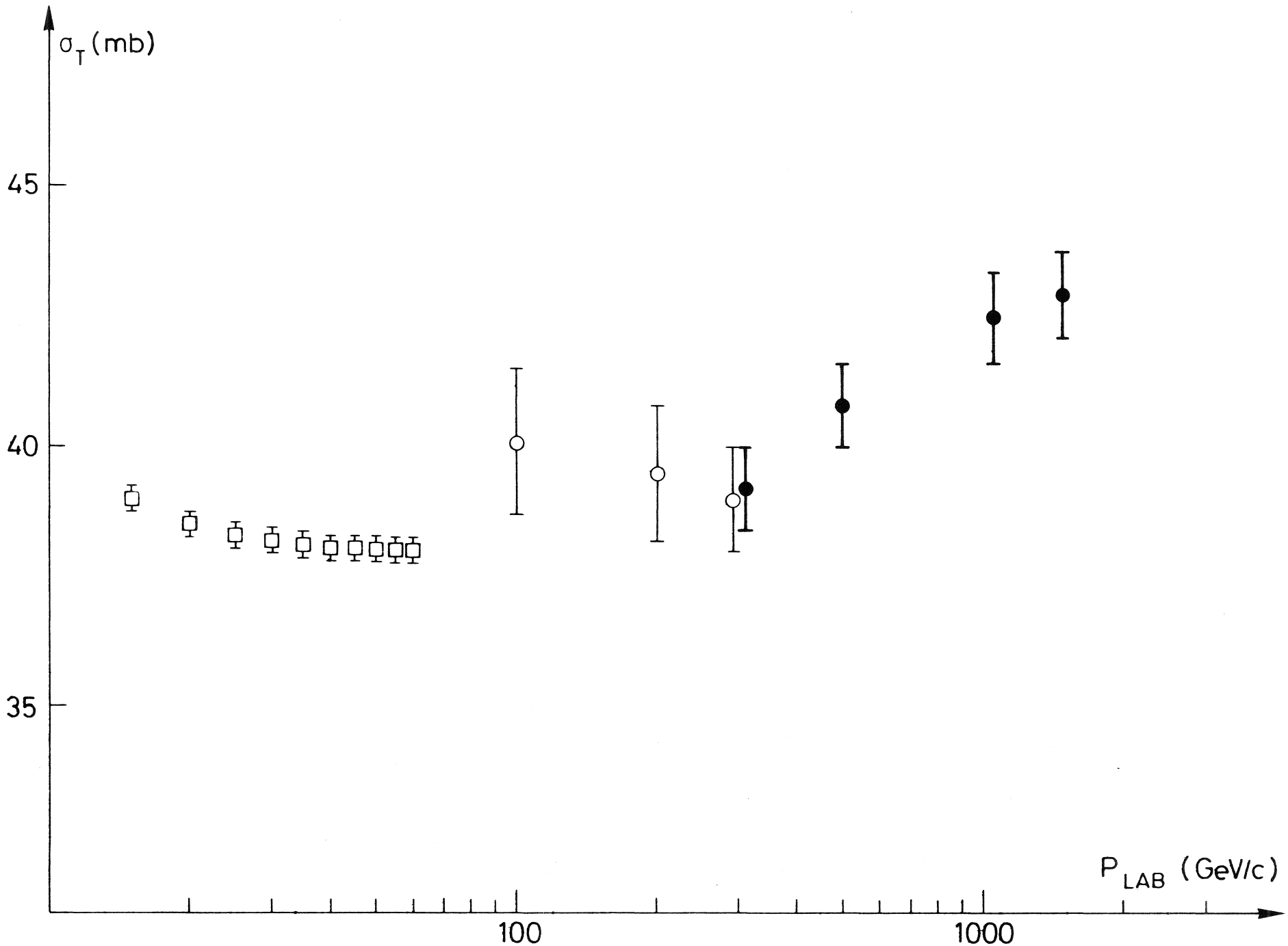

FIG. 3